THE JOURNAL OF COMPARATIVE NEUROLOGY 508:28–44 (2008)

Distinct Behaviors of Neural Stem and Progenitor Cells Underlie Cortical Neurogenesis

STEPHEN C. NOCTOR,[1]* VERÓNICA MARTÍNEZ-CERDEÑO,[1] AND ARNOLD R. KRIEGSTEIN[1,2]

[1]Department of Neurology, University of California, San Francisco, San Francisco, California 94143

[2]Institute for Regeneration Medicine, University of California, San Francisco, San Francisco, California 94143

ABSTRACT

Neocortical precursor cells undergo symmetric and asymmetric divisions while producing large numbers of diverse cortical cell types. In *Drosophila*, cleavage plane orientation dictates the inheritance of fate-determinants and the symmetry of newborn daughter cells during neuroblast cell divisions. One model for predicting daughter cell fate in the mammalian neocortex is also based on cleavage plane orientation. Precursor cell divisions with a cleavage plane orientation that is perpendicular with respect to the ventricular surface (vertical) are predicted to be symmetric, while divisions with a cleavage plane orientation that is parallel to the surface (horizontal) are predicted to be asymmetric neurogenic divisions. However, analysis of cleavage plane orientation at the ventricle suggests that the number of predicted neurogenic divisions might be insufficient to produce large amounts of cortical neurons. To understand factors that correlate with the symmetry of cell divisions, we examined rat neocortical precursor cells in situ through real-time imaging, marker analysis, and electrophysiological recordings. We find that cleavage plane orientation is more closely associated with precursor cell type than with daughter cell fate, as commonly thought. Radial glia cells in the VZ primarily divide with a vertical orientation throughout cortical development and undergo symmetric or asymmetric self-renewing divisions depending on the stage of development. In contrast, most intermediate progenitor cells divide in the subventricular zone with a horizontal orientation and produce symmetric daughter cells. We propose a model for predicting daughter cell fate that considers precursor cell type, stage of development, and the planar segregation of fate determinants. J. Comp. Neurol. 508:28–44, 2008.

Indexing terms: cortical development; ventricular zone; subventricular zone; radial glial cells; intermediate progenitor cells; precursor cells; neurogenesis; mitosis; cleavage plane; asymmetric division; symmetric division; neural stem cells; self-renewal; self-renewing divisions; mode of division

The human cerebral cortex consists of ≈50–60 billion neurons and glia (Pelvig et al., 2007), with each classified into numerous subtypes (Peters and Jones, 1984). Regulation of the mode of cell division is required to properly amplify cell numbers through symmetric divisions and diversify cell types through asymmetric cell divisions. In *Drosophila*, cleavage plane orientation plays a crucial role in determining mode of division for some, but not all, precursor cell divisions. For example, in neuroblast cells a vertically oriented cleavage within the plane of the epithelium produces symmetric daughter cells, while a horizontal cleavage orientation produces asymmetric daughter cells based on an apico-basal segregation of fate determinants (Doe, 1996). However, *Drosophila* sensory organ precursor cells also divide vertically within an epithelium, but these divisions produce asymmetric daughter

This article includes Supplementary Material available via the Internet at http://www.interscience.wiley.com/jpages/0021-9967/suppmat.

Grant sponsor: National Institutes of Health (NIH); Grant numbers: NS21223 and NS35710 (to A.R.K.).

*Current address and correspondence to: Stephen C. Noctor, PhD, UC Davis M.I.N.D. Institute, 2825 50th St., Sacramento, CA 95817. E-mail: scnoctor@ucdavis.edu

Received 18 October 2007; Revised 18 December 2008; Accepted 10 January 2008

DOI 10.1002/cne.21669

Published online in Wiley InterScience (www.interscience.wiley.com).

cells based on a planar segregation of fate determinants (Mayer et al., 2005).

Embryonic neuroepithelial cells also exhibit various cleavage plane angles during mitosis, and cleavage orientation is widely thought to dictate daughter cell fate in the embryonic neocortex in a manner similar to that described for *Drosophila* neuroblast divisions (e.g., see Langman et al., 1966; Martin, 1967; Chenn and McConnell, 1995; Haydar et al., 2003). This concept was supported by the finding that fate-determinants such as Numb display an apparent apico-basal pattern of expression that is strongest at the margin of the ventricle where cortical precursor cells divide (Zhong et al., 1996). Furthermore, examination of Numb expression in vitro shows clear segregation of the fate-determinant in dissociated cortical precursor cells prior to division (Shen et al., 2002). Thus, it was proposed that vertically oriented divisions would produce an equal partitioning of fate determinants to newborn daughter cells and, hence, a symmetric fate, while horizontally oriented divisions would produce unequal partitioning and asymmetric daughter cells (Chenn and McConnell, 1995; Zhong et al., 1996). In particular, this model specifies that horizontal divisions at the surface of the ventricle represent asymmetric neurogenic divisions: the apical daughter cell is predicted to remain proliferative in the ventricular zone (VZ), while the basal daughter is predicted to be a neuron that migrates away from the ventricle to the developing cortical plate. However, analyses of cleavage plane orientation in normal developing rodent neocortex have produced varying results (see Landrieu and Goffinet, 1979; Haydar et al., 2003), and some studies have concluded that the number of horizontal divisions at the ventricle may be insufficient to produce the large number of neurons that reside in the cerebral cortex (Sauer, 1935; Smart, 1973; Landrieu and Goffinet, 1979; Huttner and Brand, 1997). Furthermore, because of the previously unappreciated role of embryonic subventricular zone (SVZ) cells in cortical neurogenesis, the cleavage plane orientation of embryonic SVZ precursor cells has not been examined in relation to neurogenesis. This takes on added significance considering that previous studies have reported that most embryonic SVZ cells divide with a horizontal orientation (Smart, 1973; Zamenhof, 1985).

We explored the relationship between cleavage plane orientation and daughter cell fate for mitotic neuroepithelial cells in the VZ (referred to as radial glial cells), and intermediate progenitor (IP) cells in the SVZ of the embryonic rat. We demonstrate that radial glial (RG) cells divide primarily with a vertical orientation throughout development, yet switch from producing symmetric daughter cells during early stages of development to producing asymmetric daughter cells at the onset of cortical neurogenesis. Thus, RG cells exhibit a shift in the mode of division that is not accompanied by a change in cleavage plane angle, as commonly thought. We show that RG cells generate IP cells, and that most IP cells divide with a horizontal orientation while producing symmetric daughter cells. We also find that IP cells intermingle with RG cells and divide in the VZ at early stages of cortical development before the SVZ has formed. Thus, the mingling of two distinct progenitor cell types, each with its own mode of division, may better explain the shifting patterns of division and cleavage plane orientation that were previously attributed to a single precursor cell type. Finally, we show in situ that RG cells are the primary form of neural stem cell in the embryonic neocortex since they undergo self-renewing divisions and produce multiple cell types. The identification of two proliferative cell populations, one of which demonstrates neural stem cell properties in the developing brain, has potential for the application of stem cell biology to disease treatment.

MATERIALS AND METHODS

Virus preparation and animal surgery

Replication-incompetent pantropic retrovirus pseudotyped with the VSV-G glycoprotein (1×10^6 cfu/mL) carrying the enhanced green fluorescent protein (GFP) reporter gene was produced from a stably transfected packaging cell line (generous gift of Drs. Fred Gage and Theo Palmer). Embryonic day (E)15–16 rat embryos were injected with retrovirus in utero as previously described (Noctor et al., 2004). This approach labels progenitor cells that were in contact with the ventricle at the time of the retroviral injection (Walsh and Cepko, 1988). Briefly, the uterine horns of E15–16 pregnant rats were removed, cerebral hemispheres were transilluminated using a fiber optic light, and ≈0.5 μL of retrovirus was injected into the lateral ventricles of selected embryos. The uterine horns were lavaged with sterile saline, replaced, and the incision sutured. The lateral ventricle of E12 and E13 embryos was injected with retrovirus ex utero and the embryos cultured at room temperature for 2 hours in artificial cerebrospinal fluid (aCSF) bubbled with 95%/5% O_2/CO_2 containing (in mM): NaCl 125, KCl 5, NaH_2PO_4 1.25, $MgSO_4$ 1, $CaCl_2$ 2, $NaHCO_3$ 25, and glucose 20, pH 7.4, at 25°C, 310 mOsm/L. All surgical procedures were performed in accordance with the UCSF IACUC.

Organotypic slice cultures

Two hours after E12–E13 retrovirus injections, brains were removed and embedded in 4% agar. One day after E15–E16 retroviral injections embryos were sacrificed, brains removed, and embedded in 4% agar. All brains were sectioned at 375 μm on a vibratome (Leica, Deerfield, IL) in ice-chilled aerated aCSF. Slices were plated on slice culture inserts (Millicell, Millipore, Bedford, MA) in culture well plates (Corning, Corning, NY) with culture medium containing (by volume): BME 66%, Hanks 25%, FBS 5%, N-2 1%, Pen/Strep/Glutamine 1% (each from Gibco, Grand Island, NY), and d-(+)-glucose 0.66% (Sigma, St. Louis, MO). Slices remained in the culture plates for the duration of time-lapse imaging experiments and were maintained in an incubator at 37°C, 5% CO^2 between confocal imaging of the labeled cells.

Confocal time-lapse microscopy

GFP-labeled progenitor cells were imaged on an inverted Olympus (Lake Success, NY) Fluoview confocal microscope. Projection images were made from Z-stacks that included all visible processes of individual GFP+ cells, and all GFP+ clonal cells on a PC running Fluoview (Olympus). We used laser power levels that allowed us to visualize all cellular processes without risking overexposure to the live cells. Transmitted light images were taken at each timepoint to track movements of the GFP+ cells in the cultured slices. Cell position was maintained relative to the ventricular surface while RG cells maintained contact with the ventricular surface. Cells that lost contact

with the ventricular surface were positioned relative to the ventricular surface until they left the proliferative zones, at which point they were positioned relative to the pial surface for the duration of the time-lapse experiment. At some timepoints only dividing cells were imaged to reduce laser exposure to other cells in the clone. Between timepoints, slices were kept in a humidified incubator at 37°C, 5% CO_2. Cleavage plane angle of dividing GFP+ cells was measured during cytokinesis, after experiments using Adobe Photoshop v7 (San Jose, CA). The orientation of division was recorded from 0° (horizontal) to 90° (vertical) with respect to the ventricular surface. 3-Dimensional images were made from the Z-stack and the image rotated (Olympus Fluoview) to measure cleavage for cells that divided orthogonally in the slice. Montages were assembled, time-lapse sequences arranged, and images adjusted to improve contrast/brightness using Photoshop. Line drawings were prepared using Adobe Illustrator.

Morphological analysis of VZ cells

In utero injections of lower titer retrovirus (1×10^5 cfu/mL) were performed at E15, as described above, and embryos sacrificed 1 day later. Brains were perfused transcardially with chilled phosphate-buffered saline (PBS) followed by 4% paraformaldehyde (PFA, Fisher, Pittsburgh, PA). Brains were removed, fixed overnight in PFA and vibratome-sectioned at 50, 100, or 200 μm. All eGFP-labeled cells that contacted the ventricular surface were analyzed. We determined whether VZ cells had a pial directed process, and if so whether the process was restricted to the VZ, the IZ, the CP, or the MZ.

Electrophysiology

Organotypic slice cultures were transferred to a recording chamber on an Olympus BX50WI upright microscope after time-lapse recordings and were perfused with aerated aCSF. GFP+ cells were identified under epifluorescence and recordings performed using an EPC-9 patch-clamp amplifier (Heka Electronics, Canada) controlled by an Apple computer running Pulse v8.0 (Heka). Glass recording electrodes (5–7 M°) were filled with (in mM): KCl 130, NaCl 5, $CaCl_2$ 0.4, $MgCl_2$ 1, HEPES 10, pH 7.3, EGTA 1.1. Epifluorescent images of the recorded cells were collected using Scion Image (NIH, Bethesda, MD), and arranged using Photoshop. Electrophysiological responses were measured and analyzed using Pulse, and traces arranged using Igor Pro (Wavemetrics), and Freehand (Macromedia). We obtained some RG daughter cell and VZ cell recordings in acute slice preparations. Slices were prepared from embryonic rat neocortex that had been injected with eGFP retrovirus in utero as described above and 500 μM Alexa 594-conjugated biocytin (Molecular Probes, Eugene, OR) was added to identify recorded cells.

Nissl analysis

E12 embryos (n = 8) were immersion-perfused in PFA overnight at 4°C and frozen in OCT media. E15 (n = 3), E17 (n = 3), and E20 embryos (n = 3), and postnatal (P)7 neonates (n = 3) were perfused transcardially with chilled PBS followed by PFA. Brains were removed, fixed overnight in PFA, frozen in 2-methyl butane, and stored at 80°C until cryostat (Leica) sectioning at 10 μm. Sections were mounted on glass slides and stained with Cresyl Violet to label Nissl substance. Sections were photomicrographed and all anaphase and telophase cells were identified at the ventricular surface and in abventricular positions. The orientation of cleavage plane angle was calculated by averaging the angle of the sister chromatids in anaphase and telophase cells with respect to the ventricular surface. Results were statistically analyzed using Prism (Graphpad Software, San Diego, CA).

Immunohistochemistry

Coronal sections were labeled with goat polyclonal antibodies against doublecortin (DC). We tested DC antibodies that were raised in goat against the N-terminus of human doublecortin (amino acids 40–90, Santa Cruz Biotechnology, Santa Cruz, CA, #SC-8067 N-19, Lot F2204, dilution 1:100), and the C-terminus of human doublecortin (amino acids 350–402, Santa Cruz Biotechnology #SC-8066 C-18, Lot D1105, dilution 1:100), and determined that they provided comparable staining patterns. Western blotting of mouse embryo extract and 3T3-L1 doublecortin-expressing whole-cell lysate with both antibodies reveals a 40-kD band, which is consistent with the molecular weight of doublecortin protein (manufacturer's technical information). Immunoreactivity obtained with these antibodies in our hands was completely abolished through preadsorption with peptide sequences #SC-8067P, Lot O402 and #SC-8066P, Lot E059, respectively (see Fig. 6H). Coronal sections were also labeled with mouse monoclonal NeuN (Chemicon, Temecula, CA, #MAB377, clone A60, Lot #0601019159, dilution 1:1000). The NeuN antibody was raised in mouse against purified cell nuclei from mouse brain and recognizes two or three bands in the 46–48-kD range and another band at 66 kD in Western blotting (manufacturer's technical information). The NeuN antibody is reported to label most classes of neurons, and negative controls run by the manufacturer to test specificity include nonneuronal cells such as fibroblasts (manufacturer's technical information). We find that the antibody does not label any dividing cells in the embryonic neocortex, consistent with data showing that NeuN labels only neurons. Finally, we labeled coronal sections of embryonic neocortex with rabbit polyclonal Tbr2 antibodies (1:2,000; gift of Dr. Robert Hevner; see Englund et al., 2005). This antibody was generated in rabbit against the unique peptide sequence EYSKDTSKGMGAYYAFYTSP from mouse Tbr2. Western blotting of mouse brain homogenates shows a 73-kD band, matching the predicted molecular weight of Tbr2 (Quinn et al., 2007). The Tbr2 antibody does not label mature neurons and shows very little colocalization with Pax6-expressing cells in the embryonic VZ (Englund et al., 2005). Consistent with these data, we find that the Tbr2 antibody does not label RG cells (Fig. 8).

Sections were rinsed in PBS 0.1 M, pH 7.4, incubated overnight in antibody buffer containing 2% serum, 0.1% Triton X, and 0.2% gelatin diluted in PBS. Sections were rinsed, incubated with biotinylated secondary antibodies (1:100, Jackson Laboratories, West Grove, PA) for 1 hour at room temperature (RT). Sections were stained with avidin-biotin complex (Vector, Burlingame, CA) for 1 hour at RT, rinsed, and placed in 0.04% DAB (Sigma) with 0.001% H_2O_2 for 2–5 minutes. Sections were counterstained with Cresyl Violet before coverslipping with DPX (Sigma). In some cases fluorescent immunolabeling was produced using goat antimouse secondary antibodies (1:100; Jackson Laboratories) or goat antirabbit secondary

antibodies (Abcam, Cambridge, UK; 1:100). We tested the specificity of all secondary antibodies through omission of the primary antibody.

RESULTS

We labeled VZ and SVZ cortical precursor cells in rat embryonic neocortex with a low titer (1×10^5) pantropic eGFP-expressing retrovirus that was pseudotyped with the VSV-G viral coat glycoprotein (Palmer et al., 1999), which initiates virus entry into mammalian cells through interaction with ubiquitous membrane elements (Burns et al., 1993). Low retroviral titers reduced the likelihood that the fine processes of eGFP-labeled precursor cells under study would be confused with those of nearby labeled cells. We injected the retrovirus into the lateral ventricle of E12/E13 and E15/E16 rats, prepared organotypic slice cultures of sensorimotor cortex, and 24 hours after injection began recording the behaviors of proliferative eGFP+ cells (60 cells) and all progeny (129 cells total) for up to 4 days through time-lapse confocal microscopy. We documented the morphology of the labeled precursor cells and recorded their mitotic behaviors, paying close attention to interkinetic nuclear migration (IKM), cleavage plane orientation, and location of mitosis. We phenotyped newborn daughter cells based on their morphology, mitotic state, migratory behavior, and electrophysiological membrane properties when possible. Each cell division was classified as symmetric or asymmetric based on the daughter cell properties outlined above. We therefore adopted a functional definition of daughter cell symmetry based on apparent fate rather than on the inheritance of fate-determining factors.

Vertical RG cell divisions are symmetric between E13–E15

We analyzed 26 eGFP+ cells that divided during time-lapse imaging of slices prepared at E13, a stage of cortical development when neuroepithelial cells acquire the characteristics of RG cells (reviewed in Kriegstein and Götz, 2003), and when the first cortical neurons are generated (Bayer and Altman, 1991).

We identified two distinct populations of dividing cells. One set of cells (17/26) was bipolar, exhibited IKM, and divided at the surface of the ventricle. These cells matched the morphological and behavioral characteristics of RG cells (Misson et al., 1988). We analyzed the cleavage plane angle of these RG cells and found that the majority (16/17) divided with a vertical orientation (average 84° ± 1.0°^{STD}), and one (1/17) divided with a horizontal cleavage plane (8.0°). However, time-lapse imaging over several days demonstrated that both vertical and horizontal RG divisions produced symmetric daughter cells (Fig. 1, Suppl. Movies 1, 2). The majority of the RG cell divisions (9/17 divisions) produced two RG daughter cells that retained RG morphological features, resumed IKM, and divided again at the ventricular surface (Fig. 1B,C). We classified these divisions as symmetric self-renewing. Four of 17 RG divisions were apparent asymmetric self-renewing divisions, in each case producing one daughter cell that retained RG morphology, and a second set of daughter cells that included three presumed daughter neurons and one IP cell. Four additional RG divisions produced paired daughter cells that both migrated away from the ventricle.

The second group of mitotic cells (9/26) did not exhibit IKM and divided away from the ventricle. These cells often had a visible ventricular-contacting process initially, but detached from the ventricle and retracted the process prior to division. These cells matched the morphology and behavior of IP cells (Noctor et al., 2004). Most of the IP cells (5/9) divided with a horizontal orientation, and all nine IP divisions produced paired daughter cells that resembled each other in morphology and behavior (see Fig. 2A, Suppl. Movie 3). The IP daughter cells did not divide again during time-lapse imaging. These divisions were therefore classified as symmetrical terminal (see Table 1).

Vertical RG cell divisions are asymmetric between E16–E19

Following retroviral injections at E15/E16, we analyzed 34 eGFP+ cells that divided during time-lapse imaging. We recorded their morphology and behavior and that of their progeny for up to 4 days through time-lapse imaging. In this data set, 19/34 of the labeled cells had RG characteristics: bipolar cells that contacted the ventricle and pia, exhibited IKM, and divided at the ventricular surface. We measured the cleavage plane angle of the dividing RG cells and found that most (18/19), divided with a vertical cleavage plane angle (average 82.2° ± 3.8°^{STD}), and one divided at an oblique angle (57.1°).

In contrast to the vertical RG divisions that were often symmetric at early stages of cortical development, we found that between E16 and E19 most vertical RG divisions (17/18) produced asymmetric daughter cells based on the morphological, migratory, proliferative, and physiological evidence that we recorded (see Table 2).

RG cells maintained their pial fiber throughout division, as previously described (Miyata et al., 2001; Noctor et al., 2001). The pial fiber became extremely thin during metaphase but was often identifiable by conspicuous varicosities along the entire length of the fiber (Fig. 3). Many of the pial fiber varicosities traveled toward the RG cell body during metaphase and some varicosities fused with the soma before the onset of cytokinesis (see Suppl. Movies 8–10). The pial fiber was positioned above the center of the soma as the RG cells entered metaphase, but shifted laterally to one side of the vertically dividing RG cell before the cleavage furrow formed, and was inherited by one newborn daughter cell (see Fig. 4A, t = 2h:55m). Thus, vertical RG divisions produced morphologically distinct daughter cells, one of which inherited the pial fiber. We did not observe any RG divisions that were perfectly vertical (average cleavage plane angle for RG cells at early and late stages = 82.9°) and the cleavage plane angle always tilted slightly away from the daughter cell that inherited the pial fiber. In addition, we observed that the daughter cell that inherited the pial fiber began moving away from the ventricle before the daughter cell that did not inherit the fiber.

We noted different patterns of migration and proliferation for RG daughter cells that ultimately suggested asymmetric fates. Immediately after division the RG daughter cells migrated away from the ventricle at similar rates of migration, and their nuclei remained adjacent to one another in the VZ for an average 7.4 ± 2.0 hours (n = 38), and in some cases for many hours longer. Figure 4A shows an RG cell that divided vertically (t = 2h:51m) and produced daughter cells that initially moved at a similar speed. These daughter cells remained adjacent to one an-

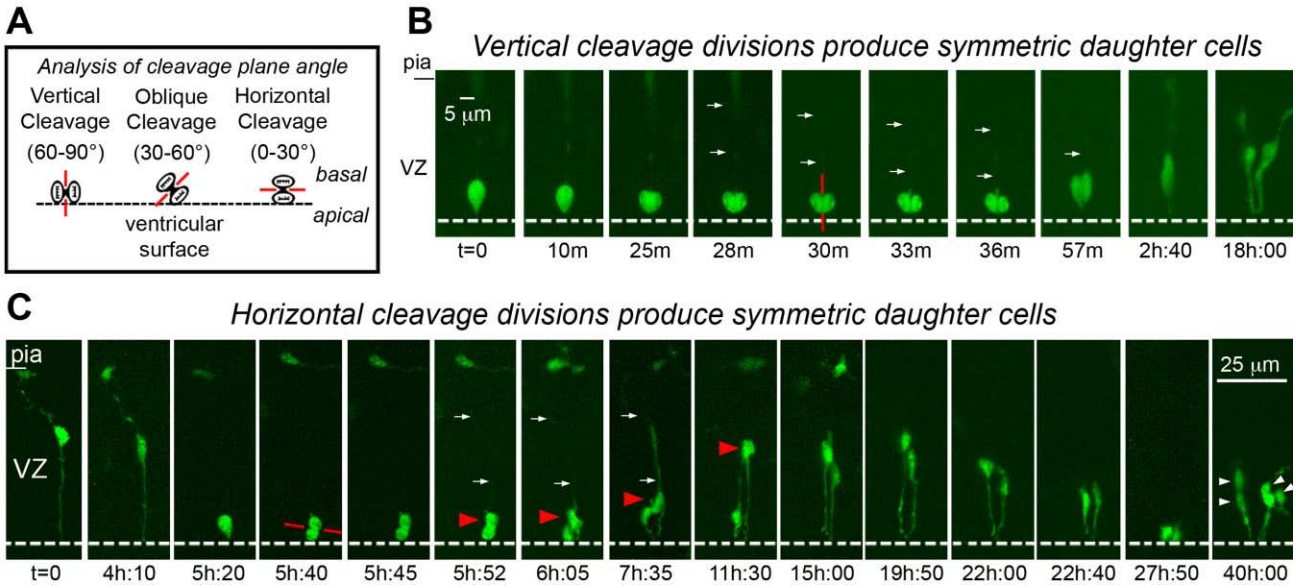

Fig. 1. Radial glial (RG) cells undergo symmetric self-renewing divisions during early stages of cortical development. **A:** Classification of cleavage plane analysis. **B:** Time-lapse imaging of a single RG cell in an organotypic slice culture prepared from an embryonic day (E)13 rat. The RG cell is shown entering metaphase at the surface of the lateral ventricle at t = 0. The dotted white line indicates the surface of the lateral ventricle. A vertically oriented cleavage furrow (red line) begins developing t = 30 m, and can be clearly visualized at t = 33 m and 36 m. Both daughter cells acquired the morphology of RG cells and remained in the ventricular zone (VZ). **C:** Horizontal cleavage plane divisions at the ventricular surface also produce daughter cells with symmetric morphologies and behaviors. A single bipolar RG cell at E13 is shown in G1-phase at t = 0. The RG cell body rose slightly in the VZ before descending to the ventricular surface (t = 5h:20m). The pial fiber became very thin and faint during mitosis but was detected post hoc (see Suppl. Movie 2). The RG cell divided with a horizontal cleavage plane (red line) at t = 5h:40m. After division the soma of the basal daughter cell (red arrowhead) moved away from the ventricle at a faster rate than its apical sibling. This behavior might be interpreted to signify an asymmetric fate for the daughter cells. Nonetheless, extended time-lapse imaging demonstrated that both daughter cells retained contact with the ventricle, resumed IKM, and divided at the ventricular surface (t = 40 h). We therefore classified this RG division as symmetric self-renewing. An unrelated cell with the morphology of a tangentially migrating cell was present in the marginal zone of the viewing field from 5–11 hours. Time elapsed is shown in either minutes (m), or hours and minutes (hh:mm) as indicated below each sequence. The entire time-lapse sequences can be viewed in Supplemental Movies 1, 2. A magenta-green version of this figure can be viewed online as Supplementary Figure 1.

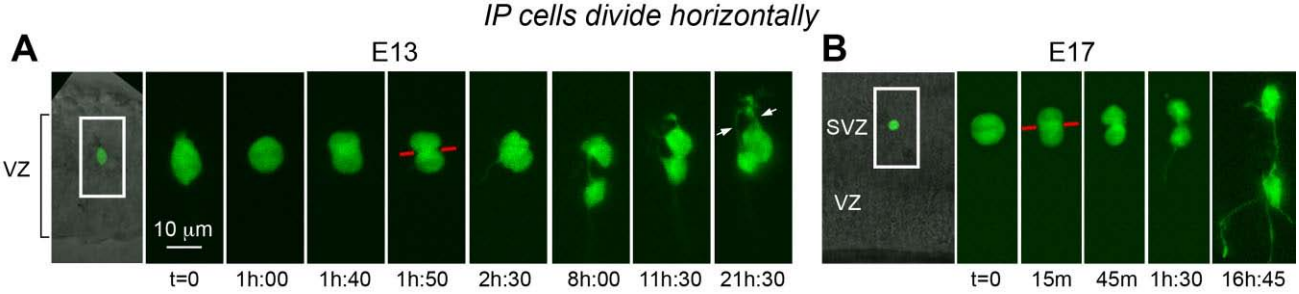

Fig. 2. Intermediate progenitor (IP) cells divide with horizontal cleavage orientation, and produce symmetric daughter cells. Time-lapse sequence of a single eGFP-labeled IP cell at embryonic day (E)13 (**A**), and E17 (**B**), that divided horizontally away from the ventricle. The left panels in both A and B are transmitted light images showing the ventricular zone (VZ), the ventricular surface, and also the pial surface in A. The IP cell shown in panel B divided in the subventricular zone (SVZ). In both examples, the IP cells divided with horizontally oriented cleavage planes (red line), and daughter cells exhibited similar morphologies and behaviors that included the extension of processes toward the ventricle (A, t = 8h; B, t = 1h:30), before the extension of a new process oriented toward the cortical plate. Time elapsed is shown in either minutes (m), or hours and minutes (hh:mm) as indicated below each sequence. The entire time-lapse sequences can be viewed in Supplemental Movies 3, 7. A magenta-green version of this figure can be viewed online as Supplementary Figure 2. Scale bar in A applies to B.

other in the VZ for nearly 24 hours, and might have been considered symmetric if cell fate was inferred by nuclear movement and position at that point (Chenn and McConnell, 1995; Haydar et al., 2003). However, extended time-lapse imaging of the eGFP-labeled cells revealed important differences. Daughter cell 2a (red arrowhead) retained RG morphology, resumed IKM, and returned to the ventricle where it divided again (Fig. 4A, t = 50h:53m). In contrast, daughter cell 2b (white arrowhead) developed a short leading process, detached from the ven-

TABLE 1. Cleavage Plane Orientation and Daughter Cell Fate of Cortical Precursor Cells in Time-Lapse Experiments at E13-E15

E13–E15 RG Cell Cleavage Plane Orientation and Daughter Cell Fate

Orientation		Average Angle	Symmetric	Asymmetric
Vertical	16	83.9°	8	8
Oblique	0	—	0	0
Horizontal	1	7.8°	1	0
Totals	17		9	8

E13–E15 IP Cell Cleavage Plane Orientation and Daughter Cell Fate

Orientation		Average Angle	Symmetric	Asymmetric
Vertical	1	61.7°	1	0
Oblique	3	44.3°	3	0
Horizontal	5	16.8°	5	0
Totals	9		9	0

Analysis of radial glial (RG) cell and intermediate progenitor (IP) cell behavior and daughter cell fate in the developing rat neocortex during time-lapse imaging between embryonic day (E)13 and E15. The number of RG cells (top panel) and IP cells (bottom panel) that divided with vertical, oblique, or horizontal orientation during time-lapse imaging is indicated. The fate of daughter cells produced by each type of division is indicated as either symmetric or asymmetric.

TABLE 2. Cleavage Plane Orientation and Daughter Cell Fate of Cortical Precursor Cells in Time-Lapse Experiments at E16-E19

E16–E19 RG Cell Cleavage Plane Orientation and Daughter Cell Fate

Orientation		Average Angle	Symmetric	Asymmetric
Vertical	18	82.2°	1	17
Oblique	1	57.1°	0	1
Horizontal	0	—	0	0
Totals	19		1	18

E16–E19 IP Cell Cleavage Plane Orientation and Daughter Cell Fate

Orientation		Average Angle	Symmetric	Asymmetric
Vertical	0	—	0	0
Oblique	0	—	0	0
Horizontal	15	8.9	15	0
Totals	15		15	0

Analysis of radial glial (RG) cell and intermediate progenitor (IP) cell behavior and daughter cell fate in the developing rat neocortex during time-lapse imaging between embryonic day (E)16 and E19. The number of RG cells (top panel) and IP cells (bottom panel) that divided with vertical, oblique, or horizontal orientation during time-lapse imaging is indicated. The fate of daughter cells produced by each type of division is indicated as either symmetric or asymmetric.

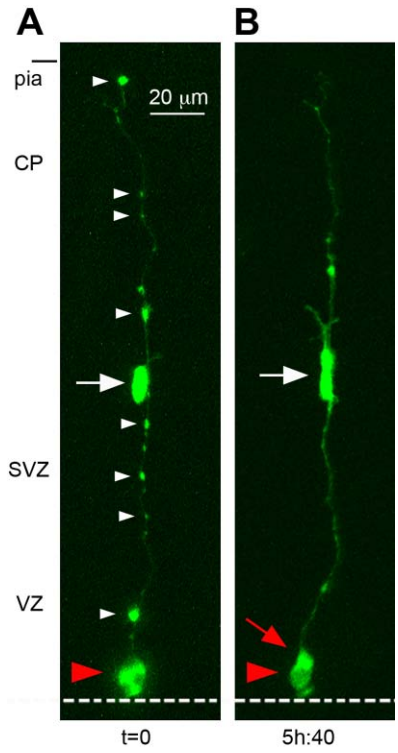

Fig. 3. The pial fiber of mitotic radial glial (RG) cells can be identified by multiple varicosities. **A:** A single RG cell (red arrowhead) is shown dividing at the surface of the ventricle at t = 0. The ventricular surface is indicated by the white dotted line, the pial surface is indicated at the top of the panel. The white arrow indicates an intermediate progenitor (IP) daughter cell apposed to its parental pial fiber. The pial fiber becomes very thin during metaphase, but is identifiable by conspicuous varicosities (white arrowheads) along the entire length of the fiber. **B:** After division the pial fiber has become thicker, and most varicosities are no longer visible. The new RG daughter cell (red arrow) is located behind its parent RG cell in this projection image. Time is shown in hours and minutes (hh:mm) below each image. VZ, ventricular zone; SVZ, subventricular zone; CP, cortical plate. A magenta-green version of this figure can be viewed online as Supplementary Figure 3.

tricle, migrated radially out of the VZ along the parental pial fiber, and divided in the intermediate zone. The morphology and behavior of cell 2b resembled that of an IP cell (Fig. 4A, Suppl. Movie 4). Vertical RG divisions that produced asymmetric daughter cells were the norm rather than the exception in the time-lapse studies performed during this stage of cortical development (see Table 2).

An examination of electrophysiological membrane properties provided additional evidence that the vertical RG divisions produced asymmetric daughter cells. After time-lapse imaging we transferred some slice cultures to an electrophysiology chamber and in four cases obtained whole-cell patch-clamp recordings from all progeny of a single RG cell. This approach allowed us to determine whether the RG cell divisions we observed in time-lapse movies produced neurons, and also whether the RG daughter cells were physiologically similar or distinct. For example, the RG cell shown in Figure 4 produced daughter cells 2a and 2b, and each daughter cell subsequently divided. Daughter cell 2b produced two similar daughter cells that resumed migration toward the cortical plate during time-lapse imaging. In addition, each daughter possessed the inward voltage-gated currents that are characteristic of immature neurons (Fig. 4A,B), and which previous studies have shown represent voltage-gated Na+ currents that produce action potentials in mature neurons (Noctor et al., 2004). In contrast, daughter cell 2a produced two daughter cells that lacked inward voltage-gated currents, instead expressing only the outward currents that are characteristic of astroglial cells in the embryonic neocortex. The site of precursor cell division (ventricular vs. abventricular), the location of daughter cells at the time of recording, or the time after division did not correlate with the presence or absence of inward voltage-gated currents. It appears that daughter cells fated to become neurons express inward voltage-gated Na+ currents soon after division, at a minimum. In our dataset we confirmed that these membrane properties are present in some daughter cells within 12 hours after division.

Nine RG divisions produced one daughter cell that remained in the VZ, and a second daughter neuron or IP cell

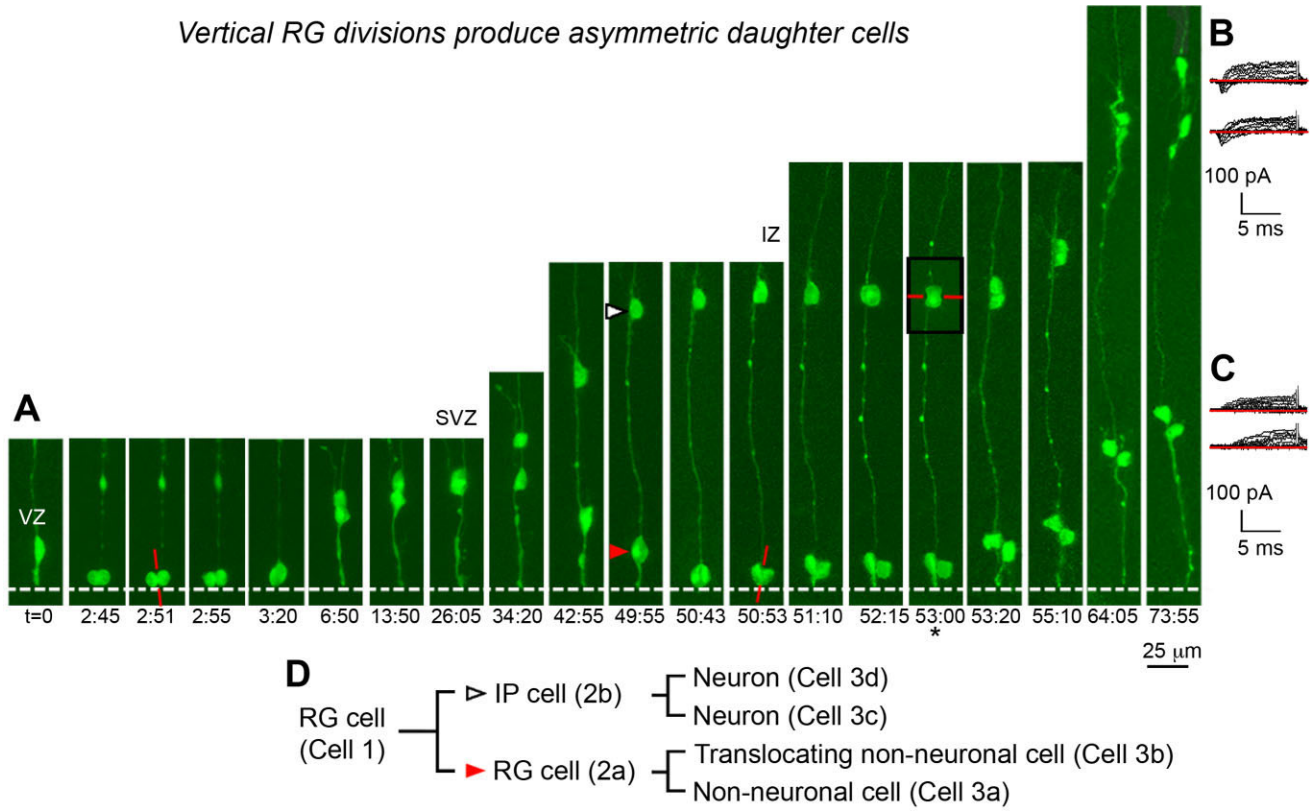

Fig. 4. Radial glial (RG) cells divide vertically at the ventricular surface to produce asymmetric daughter cells in embryonic day (E)16–E19 rat neocortex. **A:** Time-lapse imaging recorded the proliferative and migratory behaviors of one RG cell and its progeny over 3 days. The RG cell divided with a vertically oriented cleavage plane (red line) at the ventricular surface (t = 2 h: 51 m). One daughter (cell 2a, red arrowhead) was a self-renewed RG cell that resumed IKM and divided a second time at the ventricle with a vertical cleavage plane orientation (t = 50h:53m). The second daughter (cell 2b, white arrowhead) was an intermediate progenitor cell that migrated away from the ventricle along the parental RG fiber and divided with a horizontal cleavage plane orientation (red line) at the bottom limit of the intermediate zone (IZ, t = 53h). In some cases only one cell in the clone was imaged to limit exposure to laser light (asterisk). The white dotted line represents the ventricular surface. Time elapsed is shown in hours and minutes (hh:mm) below the sequence. The entire time-lapse sequence can be viewed in Supplemental Movie 4. **B:** Whole-cell patch-clamp recordings performed after time-lapse imaging demonstrated that cell 2b generated two daughter cells that both expressed the inward voltage-gated currents (downward deflection of traces below red line) that are characteristic of sodium currents in immature neurons. **C:** In contrast, cell 2a produced two daughter cells that lacked inward voltage-gated currents, exhibiting only the outward voltage-gated currents that are characteristic of potassium currents in astroglial cells. **D:** Lineage tree depicting the progeny of the single RG cell shown in panel A. VZ, ventricular zone; IZ, intermediate zone. A magenta-green version of this figure can be viewed online as Supplementary Figure 4.

that migrated out of the VZ. Because the daughter cell that remained in the VZ retained RG morphology, resumed IKM, and divided at the ventricular surface, we identified these daughter cells as self-renewed RG cells. Nine additional RG divisions produced one daughter cell that inherited the pial process after division, detached from the ventricle, and migrated toward the cortical plate through translocation along the inherited pial fiber. In these cases the second daughter cell migrated in the same direction through locomotion. In these cases the daughter cells that inherited the pial fiber and translocated toward the pia often remained proliferative as they migrated away from the ventricle, in one case dividing two additional times during translocation (Suppl. Movies 5, 6). We tested the identity of daughter cells produced by translocating cells and found that they were not neuronal based on the lack of inward voltage gated currents (see Suppl. Movie 5). This physiological profile suggests an astroglial fate for the translocating cells, and is consistent with previous findings that during late stages of neurogenesis translocating cells in rodent and human developing neocortex do not express neuronal markers (deAzevedo et al., 2003; Noctor et al., 2004), and transform into astrocytes (Schmechel and Rakic, 1979). However, our results suggest that neuronal and glial producing RG cells are not restricted to separate lineages. We observed individual RG cells that generated IP cells or neurons first, followed by a translocating daughter that remained proliferative and generated nonneuronal daughter cells (Fig. 4). Together, these data demonstrate that in addition to undergoing self-renewing divisions, individual RG cells also produce multiple cell types, including additional RG cells, neurons, IP cells, and astroglial cells.

The length of the RG cell cycle was slightly shorter during time-lapse recording at earlier stages of development, as previously reported for VZ precursor cells (Takahashi et al., 1995b). Within the RG cell population there may be a correlation between cell cycle time and mode of

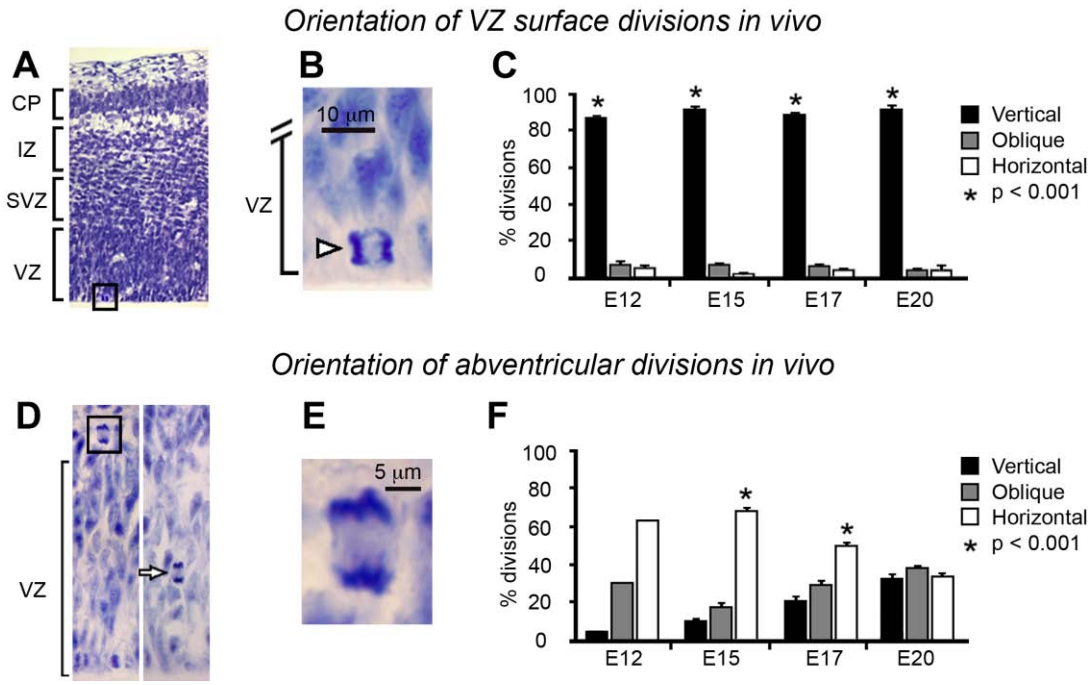

Fig. 5. Nissl analysis demonstrates that in vivo the majority of ventricular zone (VZ) surface divisions occur with a vertical cleavage plane orientation (**A–C**), and that the majority of abventricular divisions in the subventricular zone occur with a horizontal orientation (**D–F**). A: Nissl-stained tissue prepared from the neocortex of an embryonic day (E)17 rat. B: Higher power image showing a dividing precursor cell at the surface of the VZ. C: The percentage of ventricular surface divisions with vertical cleavage plane (black bars), oblique (gray bars), or horizontal (white bars) orientation did not change during cortical development. D: Nissl-stained tissue prepared from an E15 rat showing two examples of abventricular progenitor cells undergoing division away from the ventricle (arrow). E: Higher-power magnification of the boxed region in (D). F: The percentage of abventricular mitoses with vertical cleavage plane (black bars), oblique (gray bars), or horizontal (white bars) orientation changed across the period of cortical neurogenesis. Significantly more abventricular cells divided with a horizontal orientation at E15 and E17 (asterisk, $P < 0.01$), compared to either horizontal or oblique divisions. But the orientation of the abventricular mitoses was random at the end of neurogenesis at E20. Error bars depict the standard error of the mean. IZ, intermediate zone; CP, cortical plate.

division since early RG cell cycle time was shorter, and these divisions were more likely to be symmetric. However, there does not appear to be a relationship between cell cycle length and mode of division within the IP cell population. The IP cell divisions we recorded were symmetric regardless of cell cycle length (ranging from 19 to 48 hours). This evidence suggests that progenitor cell type must be factored into correlations between mitotic behaviors and mode of division.

Previous studies have reported a transient increase in the proportion of horizontal divisions at the surface of the lateral ventricle around mid-neurogenesis (Chenn and McConnell, 1995; Haydar et al., 2003; Sanada and Tsai, 2005). However, we observed only one horizontal division during time-lapse imaging of surface dividing VZ cells (1/36 RG cell divisions). We tested whether our in situ time-lapse results reflect precursor cell behavior in vivo. We quantified the proportion of surface dividing precursor cells that divided with vertical, horizontal, or oblique orientations in fixed coronal sections of embryonic rat neocortex. Vertical divisions were predominant at the VZ surface at each stage of development we examined (n = 1592 cells; see Fig. 5A–C). The proportion of vertical divisions did not change, remaining at ≈90% throughout development (analysis of variance [ANOVA], $P < 0.001$; Table 3). These results are consistent with previous examinations of neuroepithelial cell mitoses (Sauer, 1935; Fujita, 1960; Langman et al., 1966; Hinds and Ruffett, 1971; Smart, 1973; Zamenhof, 1987; Bayer and Altman, 1991; Adams, 1996; Reznikov et al., 1997; Kamei et al., 1998; LoTurco et al., 2003; Weissman et al., 2003; Kosodo et al., 2004), and in particular with those studies that found no change in cleavage plane angle of surface dividing precursor cells during cortical development (see Landrieu and Goffinet, 1979).

Horizontal IP cell divisions are symmetric between E16–E19

We found very few horizontal divisions at the ventricle throughout cortical development. During time-lapse imaging of slices prepared from embryonic rats after E15/16 retroviral injections, 15/34 eGFP labeled cells divided away from the ventricle. Abventricular mitoses in the embryonic neocortex have been described in previous studies (e.g., Hamilton, 1901; Smart, 1961), but have received more attention recently following the demonstration that they produce neurons (Tarabykin et al., 2001; Smart et al., 2002; Haubensak et al., 2004; Miyata et al., 2004; Noctor et al., 2004). None of the abventricular cells exhibited IKM, and each cell retracted all visible processes prior to division (Fig. 2B, Suppl. Movie 7), matching IP cell behavior (Noctor et al., 2004). In some experiments (n = 9)

TABLE 3. Proportion of Mitotic Cells That Divide with Vertical, Oblique, or Horizontal Cleavage Plane Orientations at the Ventricular Surface and Away from the Ventricle In Vivo

Ventricular Surface Divisions In Vivo				
	E12	E15	E17	E20
Vertical	86.15% (224)	92.87% (456)	89.94% (572)	92.20% (189)
Oblique	7.69% (20)	5.50% (27)	6.13% (39)	3.90% (8)
Horizontal	6.16% (16)	1.63% (8)	3.93% (25)	3.90% (8)
Number of cells counted	n = 260	n = 491	n = 636	n = 205
Number of animals	8	3	3	3

Abventricular Divisions In Vivo					
	E12	E15	E17	E20	P7
Vertical	6.25% (1)	11.17% (22)	21.80% (75)	30.68% (54)	31.51% (46)
Oblique	31.25% (5)	19.29% (38)	27.62% (95)	37.50% (66)	39.73% (58)
Horizontal	62.50% (10)	69.54% (137)	50.58% (174)	31.82% (56)	28.76% (42)
Number of cells counted	n = 16	n = 197	n = 344	n = 176	n = 146
Number of animals	8	3	3	3	3

The proportion of ventricular surface and abventricular mitoses with vertical, oblique, or horizontal cleavage plane orientation was recorded in Nissl-stained tissue prepared from rats at embryonic day (E)12, E15, E17, E20 and postnatal day 7 (P7). Only mitotic cells in anaphase or telophase were included for analysis. The number of progenitor cells that divided at each orientation is included in parentheses. The total number of mitoses counted, and the number of animals analyzed at each age is indicated in the bottom rows.

we observed RG divisions that produced IP cells (see Fig. 4A). In these cases the newborn IP cells migrated radially away from the ventricle along the parental pial fiber, detached from the ventricle and divided at a distance from the ventricular margin (15–165 μm). Notably we found that most IP cells divided with a horizontal cleavage plane (average angle 8.9° ± 6.8°^{STD}). Finally, in each time-lapse observation, IP divisions produced daughter cells that exhibited similar morphologies and behaviors after division (n = 15 divisions). In addition, whole-cell patch-clamp recordings from both daughter cells after two IP divisions provided further evidence that IP divisions produce symmetric daughter cells: in each case both daughter cells possessed the inward voltage-gated currents that are characteristic of immature neurons (Fig. 4A,B). We compared the orientation of dividing cells in our time-lapse movies with that of IP cells in vivo and found that in vivo the majority of abventricular cells also divided with a horizontal cleavage plane, especially during peak periods of neurogenesis. But that after cortical neurogenesis was complete, and after RG cells had exited the VZ and transformed into astroglial cells, the orientation of IP cells was random (n = 541 cells, Fig. 5D–F).

Embryonic SVZ is a neurogenic compartment

The embryonic SVZ was long thought to be a gliogenic compartment (e.g., Privat, 1975). But since we observed neurogenic divisions during time-lapse imaging we asked what proportion of embryonic SVZ mitoses were neurogenic by costaining tissue with antibodies directed against doublecortin (DC) protein and for Nissl substance. DC antibodies are widely used to label immature and migrating neurons, but DC also labels proliferating neural precursor cells in the subgranular zone of the adult hippocampus (Brown et al., 2003; Kempermann et al., 2004). DC antibodies densely label the embryonic cortical plate and IZ (Fig. 6A), but we also observed numerous DC+ cells undergoing division at a distance from the ventricular surface (Fig. 6C–6F). We quantified the percent of abventricular dividing cells that expressed DC and found that during embryonic ages the vast majority of abventricular dividing cells expressed DC (602/710 mitoses). At E12 93% of abventricular mitoses were DC+, and the percent of DC+ abventricular mitoses fell slightly to 83% by E20 (Fig. 6B). As a control we preadsorbed DC antibodies with a DC protein peptide sequence and found this abolished immunoreactivity (Fig. 6H). We also costained one set of slices with antibodies directed against the mature neuronal marker NeuN and found that mitotic SVZ cells were not labeled with NeuN antibody (0/123 cells at E17, data not shown). The expression of DC by most embryonic abventricular mitotic cells suggests that the eGFP+ SVZ progenitor cells in our time-lapse experiments represented neuronal progenitor cells, an interpretation supported by the electrophysiological recordings we obtained from some IP daughter cells. DC expression by IP cells may simply reflect commitment to a neuronal lineage. But DC is essential for neuronal migration (des Portes et al., 1998; Gleeson et al., 1998), and plays a crucial role in movement of the nucleus (Tanaka et al., 2004), and leading process extension (Schaar et al., 2004). Since IP cells extend a leading process and migrate radially toward the cortical plate, the expression of DC suggests that this protein may also be involved with the migration of IP cells.

IP cell distribution changes during cortical development

Previous studies have shown that some abventricular cells divide very close to the ventricle (Takahashi et al., 1993), and that RG cells and IP cells intermingle in the VZ (Takahashi et al., 1995a). Because IP cells can divide near the site of RG cell division, and because we find that they are more likely to divide with a horizontal orientation than RG cells, we examined the distribution of IP cells during development to determine if this might contribute to perceived changes in the patterns of cleavage plane orientation.

We used an antibody directed against the transcription factor Tbr2 that is expressed by cortical IP cells (Englund et al., 2005), and at E12 found that a small number of Tbr2+ cells were present in the neocortex. At this stage of development the cortex is only 60–70 μm thick and most

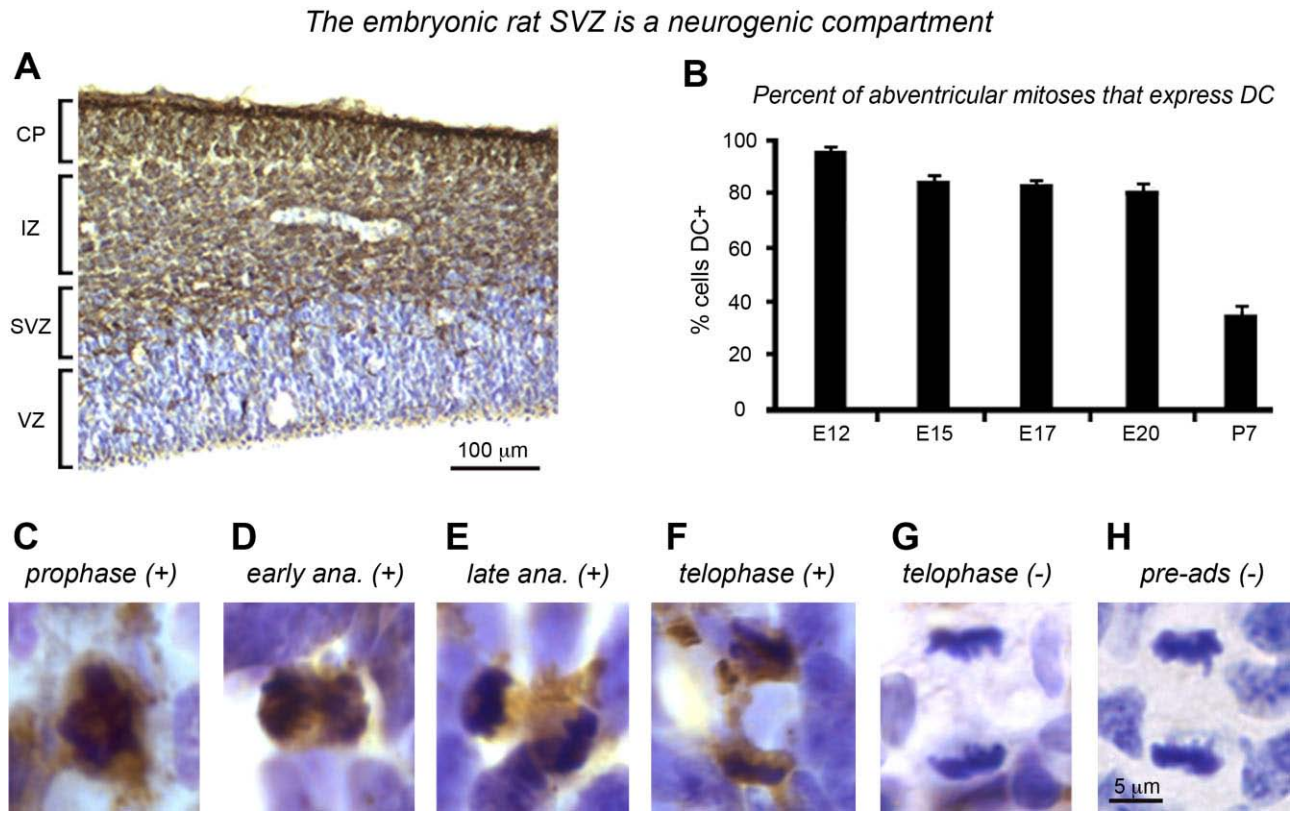

Fig. 6. The embryonic subventricular zone (SVZ) is a neurogenic compartment. **A:** Nissl-stained tissue costained with doublecortin (DC) antibodies shows the pattern of DC-immunoreactivity in a coronal section of E17 rat cortex. The cortical plate (CP) is densely labeled while the ventricular zone (VZ) is lightly stained. **B:** Histogram showing the proportion of mitotic abventricular cells that express DC during embryonic cortical development. At E12 93% of SVZ mitoses are DC+. The proportion of DC+ mitoses decreased slightly to 83% at E20. By P7 the proportion of DC+ mitoses has fallen to less than 40%. Error bars depict the standard error of the mean. **C–F:** DC antibodies label abventricular mitoses. DC+ abventricular cells are shown in prophase, early anaphase, late anaphase, and telophase. **G:** Not all abventricular mitotic cells expressed DC. A telophase abventricular mitosis that does not express DC is shown. Brown DC-immunoreactive product can be seen in neighboring cells. **H:** Preadsorption of the doublecortin (DC) antibody with DC protein eliminated immunostaining. IZ, intermediate zone; SVZ, subventricular zone.

Tbr2+ cells were located in the upper portion of the VZ at an average distance of 57.1 ± 3.4 μm from the lumen surface (n = 89 cells, four animals, Fig. 7A,E).

E15 corresponds to the stage of cortical development when the SVZ begins to form (Bayer and Altman, 1991), and at this stage the number of Tbr2+ cells significantly increased. The Tbr2+ cells were more evenly distributed throughout the VZ than they were at E12. Many Tbr2+ cells were located very close to the ventricle (Fig. 7B,F,J), and greater than 25% of all Tbr2+ cells were located within 40 μm of the ventricle at E15 (n = 655 cells, three animals). We examined ventricular mitoses with Syto-11 counterstaining and found that Tbr2+ cells accounted for nearly 7% of the mitotic figures at the ventricular margin at E15 (n = 21/304 cells). In some cases we observed Tbr2-positive and -negative mitotic cells adjacent to one another at the margin of the ventricle (Fig. 7L).

By E17 in the rat neocortex the SVZ can be clearly distinguished from the VZ and we found that the Tbr2+ population of cells had shifted away from the ventricle to reside within this newly formed compartment. Only 1.2% of Tbr2+ cells were located within 40 μm of the surface (Fig. 7C,G; n = 1267 cells, three animals). In addition, we examined the ventricular surface mitoses with Syto-11 staining and found that only 2/543 expressed Tbr2.

At the end of cortical neurogenesis, E20, Tbr2+ cells were concentrated within the SVZ (Fig. 7D,H), and we did not observe any Tbr2+ cells at or near the ventricle (n = 1298 cells, three animals).

RG cells do not express Tbr2. Since we observed some Tbr2-positive cells at the ventricular margin where RG cells divide, we asked whether a subset of RG cells might express Tbr2. We labeled precursor cells with the eGFP-expressing retrovirus at E15 and counterstained fixed tissue with Tbr2 antibodies. We noted intense Tbr2 expression in IP cells as expected, but did not observe Tbr2 expression in any RG cells (n = 48 radial clones, Fig. 8).

Tbr2+ cells divide with a horizontal orientation. Since we found that most IP cells divided horizontally, and that during SVZ formation many Tbr2+ cells are found close to the ventricle, we asked whether the appearance of IP cells in the neocortex at E15 could produce an apparent increase in the proportion of horizontal divisions near the ventricle. We measured cleavage plane orientation of Tbr2+ cells that were in anaphase or telophase and found

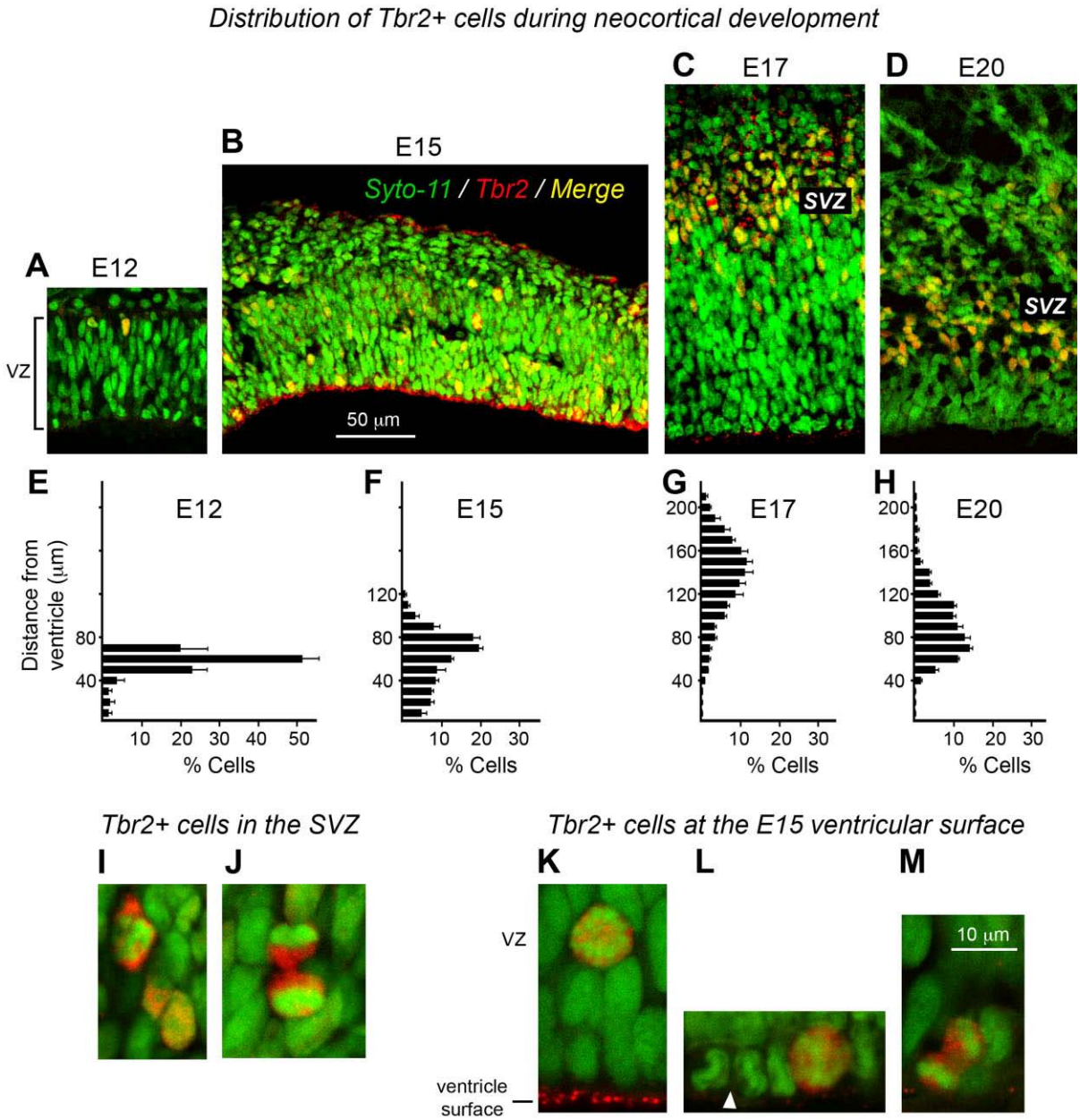

Fig. 7. Tbr2+ intermediate progenitor (IP) cells are located in the ventricular zone (VZ) before the subventricular zone (SVZ) forms. **A:** The nuclear transcription factor Tbr2 (red) is detected in a few cells at embryonic day (E)12. Syto-11 (green) labels the chromatin of all cells. Interphase IP cells with dispersed chromatin that express Tbr2 appear yellow. **B:** At E15 the number of Tbr2+ cells increases dramatically throughout the VZ. Many Tbr2+ cells are close to the ventricle and some Tbr2+ mitoses can be seen at the VZ surface. **C:** By E17 the SVZ has fully formed and the majority of Tbr2+ cells are concentrated in the SVZ. Mitotic Tbr2+ cells are no longer present at or near the ventricle. **D:** The VZ has shrunk considerably by the end of cortical neurogenesis at E20. Tbr2+ cells are detected in the SVZ, but not in the VZ. **E–H:** The position of Tbr2+ cells in the proliferative zones of embryonic neocortex is plotted in these graphs. The distance of Tbr2+ cells was measured in a series of 10-μm bins from the VZ surface to the pia. The Y-axis depicts distance from the ventricle, the X-axis depicts the proportion of Tbr2+ cells that were present in each 10 μm bin. Error bars represent the standard error of the mean. The proportion of Tbr2+ cells undergoing division at the ventricle or near the surface of the ventricle is much higher at E15 (F), in comparison to the proportion earlier at E12 (E), or later at E17 (G). **I:** Examples of Tbr2+ cells are shown in the embryonic SVZ. **J:** A Tbr2-positive cell in the SVZ in telophase. Tbr2-immunoreactivity (red) is present between the sister chromatids. **K–M:** Examples of Tbr2+ cells undergoing division at the ventricle in the E15 rat. K: A Tbr2+ cell in prophase entering mitosis in near the VZ surface. L: A Tbr2+ cell in prophase at the surface of the VZ. The white arrowhead points to an adjacent Tbr2–negative cells undergoing division at the VZ surface. M, A Tbr2+ cell is at the margin of the ventricle undergoing division with an oblique orientation. A magenta-green version of this figure can be viewed online as Supplementary Figure 5. Scale bar in B refers to A–D; scale bar in M refers to I–L.

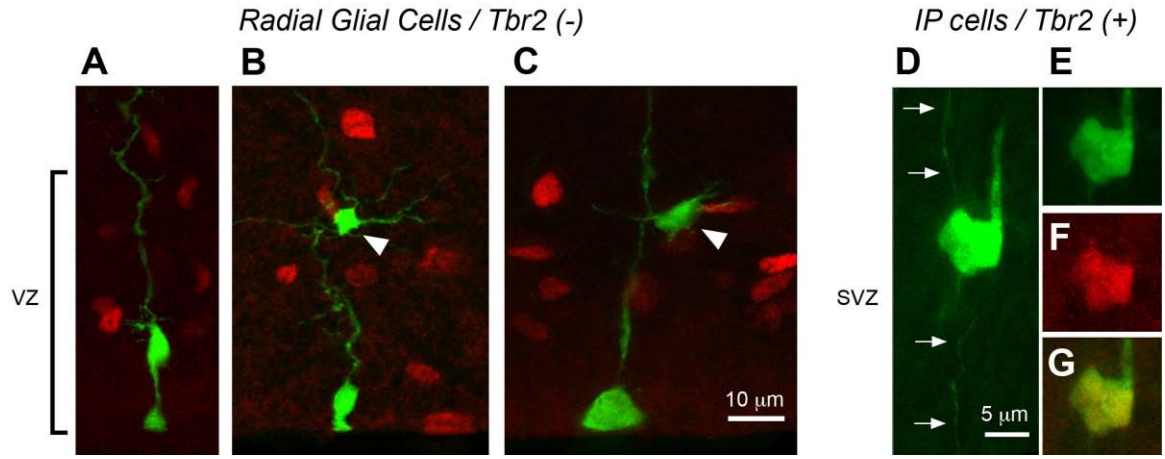

Fig. 8. Radial glial (RG) cells do not express Tbr2. **A–C:** GFP-labeled RG cells (green) in the embryonic ventricular zone (VZ) do not express Tbr2 (red). RG cells in interphase (A), G-2 phase (B), and prophase (C). Only RG daughter cells that are intermediate progenitor (IP) cells express Tbr2. The Tbr2 negative daughter cells (white arrowheads) may represent daughter neurons that are produced by RG divisions. **D:** A GFP-labeled IP cell in the subventricular zone migrating along its parental RG fiber (white arrows). **E:** The same cell shown in panel D expresses Tbr2 (red, **F**). **G:** Merged image showing colocalization. A magenta-green version of this figure can be viewed online as Supplementary Figure 6.

that the majority divided with a horizontal orientation, specifically during peak stages of neurogenesis. At E15, 75.0 ± 7.2% of Tbr2+ cells divided horizontally (n = 55 cells, three animals), and at E17 58.5 ± 5.9% of Tbr2+ cells divided horizontally (n = 174 cells, three animals).

DISCUSSION

RG cleavage plane is not associated with mode of division

We show here that the vast majority of RG cells divide with a vertical cleavage plane orientation throughout cortical development, and that vertical RG divisions produce symmetric daughter cells during early stages of cortical development and asymmetric daughter cells during later stages. Thus, the RG cell mode of division changes from symmetric to asymmetric at the start of neurogenesis, but this is not correlated with a switch in cleavage plane orientation as commonly thought. Changes in cleavage plane play a prominent role in daughter cell fate in some invertebrate systems such as the *Drosophila* neuroblast cell, and a similar model has been proposed for predicting daughter cell fate in the developing neocortex (Langman et al., 1966; Martin, 1967; Chenn and McConnell, 1995; Haydar et al., 2003). However, *Drosophila* neuroblast cells delaminate from the neuroectoderm before dividing horizontally, have an asymmetrically positioned mitotic spindle, and produce unequally sized daughter cells (Betschinger and Knoblich, 2004). RG cells do not share these characteristics; they remain embedded in the neuroepithelium throughout the cell cycle, divide vertically, have a centrally positioned mitotic spindle, and produce daughter cells that are of equal size. The behavior of *Drosophila* sensory organ precursor cells, which divide vertically while producing asymmetric daughter cells, may provide a better match for RG behavior and may serve as better models for understanding mechanisms that promote asymmetric division in RG cells. Planar segregation of fate determinants, rather than apico-basal segregation, plays a deciding role in sensory organ precursor cell divisions. Our finding that vertical RG divisions produce asymmetric daughter cells suggests that this may also be true in the mammalian VZ. Our results do not preclude the asymmetric segregation of fate determinants along the apico-basal axis in horizontally dividing RG cells. But since vertical divisions outnumber horizontal divisions by ≈18:1, even during stages of cortical development when nearly 50% of RG divisions are asymmetric (Mione et al., 1997; Cai et al., 2002), we propose that planar segregation of fate determinants represents a more common mechanism for producing asymmetric RG divisions in the embryonic neocortex. Our finding that vertical cleavage plane divisions at the ventricular surface produce asymmetric daughter cells in the developing cerebral cortex is consistent with studies performed in developing rat and chick retina (Tibber et al., 2004), zebrafish retina (Das et al., 2003; Poggi et al., 2005; Zolessi et al., 2006), and zebrafish hindbrain (Lyons et al., 2003), showing that vertical divisions produce asymmetric daughter cells. Those results together with our findings demonstrate that cell fate symmetry in the vertebrate central nervous system cannot be strictly predicted based solely on the orientation of the mitotic cleavage plane.

Orientation of the mitotic spindle plays a crucial role in determining which cellular components will be inherited by nascent daughter cells, especially in invertebrate systems (see Wodarz, 2005). Previous studies have shown that the spindle in mammalian neocortex rotates prior to division, as if 'searching' for proper alignment prior to division (Adams, 1996; Haydar et al., 2003). Regulation of the mitotic spindle is commonly understood to signify vertical versus horizontal orientations in dividing cells. However, we find that vertically oriented divisions can produce either symmetric or asymmetric daughter cells, and that both vertically and horizontally oriented divisions can produce symmetric daughters. The consistent,

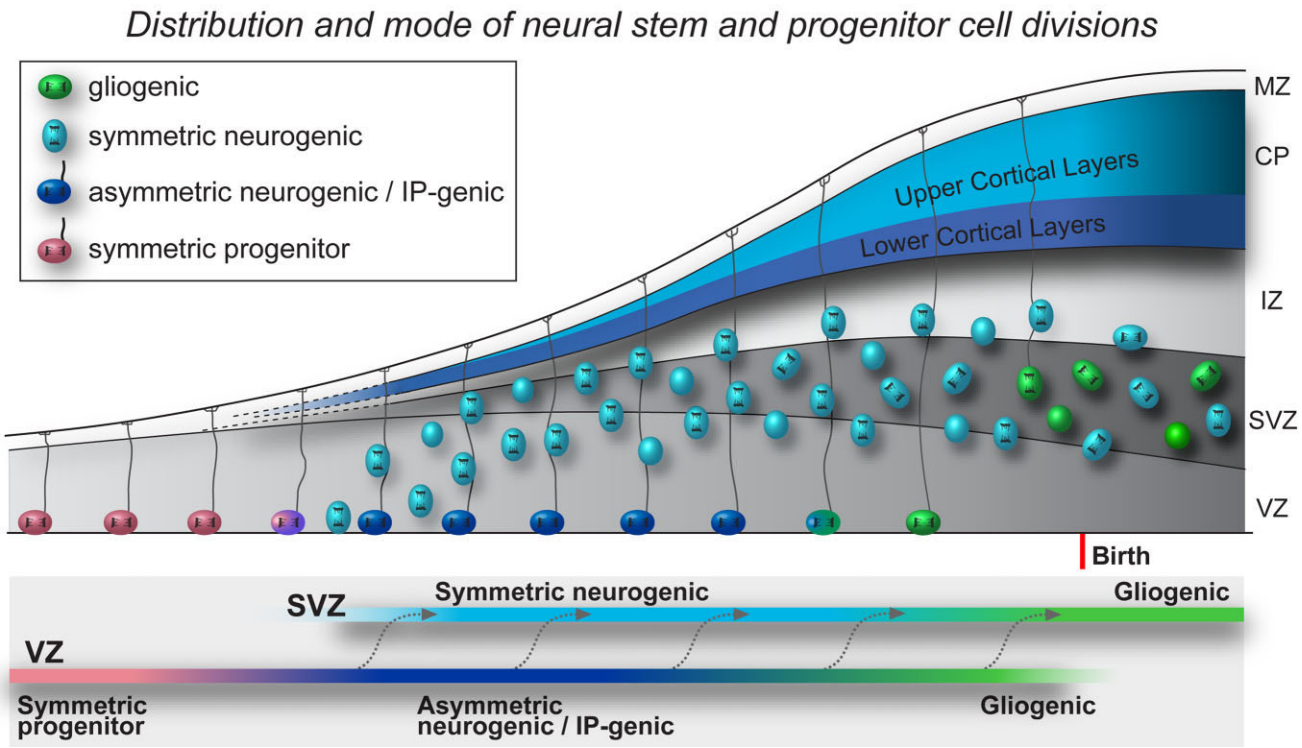

Fig. 9. The location, cleavage plane orientation, and mode of neural stem and progenitor cell divisions in the dorsal telencephalon during cortical development. Radial glial (RG) cells divide vertically at the surface of the ventricular zone (VZ) throughout cortical development. Before neurogenesis begins most RG divisions are symmetric self-renewing (red), expanding the founder population of VZ progenitor cells. At the onset of neurogenesis RG cells undergo asymmetric self-renewing divisions (dark blue) that produce either neurons or intermediate progenitor (IP) cells. Daughter neurons produced directly by RG cells may form the lower cortical layers. RG cells produce IP cells throughout the remainder of cortical neurogenesis. Daughter IP cells (light blue) divide close the ventricle during early stages of neurogenesis, but their location shifts away from the ventricle and the IP cells divide in the subventricular zone (SVZ) once that structure has formed. Most IP cells divide horizontally and produce symmetric pairs of neurons that form the upper cortical layers. After producing neurons RG cells translocate away from the ventricle and produce glial progeny (green). IZ, intermediate zone; MZ, marginal zone.

high proportion of radial glial cells that divide with a vertical orientation indicates that spindle orientation is uniformly regulated in mitotic RG cells throughout cortical development. A recent study has reported that mammalian G-protein subunits regulate spindle orientation in the developing neocortex and alter the symmetry of precursor cell divisions (Sanada and Tsai, 2005), but this study did not distinguish between RG and IP cells, and may have missed the important differences exhibited by these two cell types. We distinguished the behaviors of RG and IP cells, and include an analysis of neurogenic IP cells that were not considered in previous studies of fate determination. We show that RG and IP cells divide with cleavage plane orientations that are largely perpendicular with respect to one another, and exhibit different modes of division. Furthermore, we demonstrate that IP cells intermingle with RG cells in the VZ at early stages of development, but that IP cells become concentrated away from the ventricle in the SVZ as this structure forms. We propose that the appearance of IP cells in the VZ at early stages of neurogenesis may account for the temporary increase in horizontal divisions that have been reported in some studies (Chenn and McConnell, 1995; Haydar et al., 2003; Sanada and Tsai, 2005). The increase in the number of IP cells that divide close the ventricle was not sufficient to significantly increase the number of horizontal divisions at the ventricular margin, but produces a significant increase in horizontal divisions when surveying the region of the VZ within 40 microns of the surface. Mitotic IP cells are largely found in the SVZ, but also undergo division in the VZ and the IZ. This has been noted in previous publications (e.g., Takahashi et al., 1993), and was also highlighted in a recent publication (Carney et al., 2007). Thus, the mingling of IP and RG cells in the VZ, each with its own mode of division, and the changing distribution of IP cells explains the shifting patterns of division and cleavage plane orientation that was previously attributed to a single precursor cell type (Fig. 9).

Our results are potentially consistent with a model proposed by Huttner and colleagues (Kosodo et al., 2004), which predicts that inheritance of apical plasma membrane dictates symmetric or asymmetric daughter cell fate. In this model vertically oriented divisions are predicted to equally split the apical plasma membrane of the mitotic cell and produce symmetrically fated daughter cells, whereas a minor change in cleavage plane angle is predicted to produce unequal inheritance of apical plasma membrane, and hence asymmetrically fated daughter cells. In our time-lapse experiments most RG cells divided with an orientation slightly off vertical (average 82.9°), which would be predicted to be asymmetric if cleavage plane angle influenced the inheritance of apical plasma.

However, some of these divisions were symmetric, particularly during earlier stages of cortical development. In addition, we observed a rare horizontal division at the ventricular surface in which only the apical daughter cell appeared to contact the ventricle, yet this division produced symmetric daughter cells. In this case, both apical and basal daughter cells may have maintained contact with the ventricular surface after division, indicating that maintenance of contact with the ventricle, and perhaps inheritance of apical plasma, may not be determined in a strict apico-basal fashion that can be predicted by measuring the apparent cleavage plane orientation of surface dividing precursor cells. Future studies should determine whether, and for how long, newborn daughter cells maintain contact with the ventricle after divisions, and how this influences their ultimate fate.

The mode of division in the SVZ is likely regulated through distinct mechanisms. IP cells appear to retract the process that contacts the ventricle prior to division, suggesting perhaps that these cells may not inherit or parse apical plasma. While the IP cells mostly undergo symmetric divisions, we observed both symmetric terminal and symmetric proliferative IP cell divisions. Our results show that the cleavage plane orientation of IP cells is largely horizontal with respect to the ventricular surface, but perhaps more interestingly, is perpendicular to the trajectory of the pial fiber upon which they migrate. This suggests the possibility that affiliation with the parental RG fiber may influence cleavage plane orientation of IP cells. This idea is further supported by our observation that IP cell cleavage orientation is horizontal during embryonic neurogenesis when RG pial fibers are present, but becomes random after cortical neurogenesis is complete, and RG pial fibers are no longer present in the neocortex. Our data suggest that the cleavage plane orientation of IP cell division is not an important feature in determining daughter cell fate. Finally, we observed IP cells with short leading processes that migrated radially toward the cortical plate along pial fibers, and found that IP cells express the neuronal lineage marker doublecortin. This indicates that the classification of embryonic cortical cells as neurons based on their morphology, affiliation with RG pial fibers, or expression characteristics is not sufficient.

Precursor cell morphology and mode of division

The striking difference in the morphology and behavior of RG and IP cells suggests that RG cell morphological features could play an important role in signaling pathways involved in regulating the mode of division and daughter cell fate. RG cells maintain attachments to both the ventricular and pial surfaces, but IP cells do not. The ventricular and pial processes may provide RG cells with access to intercellular signals that are not available to IP cells, and could be an important factor in maintaining a self-renewing 'stem-cell' population. For example, β-catenin, which is associated with RG ventricular endfeet, appears to prevent cell cycle exit and maintains VZ cells in a proliferative state (Chenn and Walsh, 2002). The RG ventricular endfeet also express proteins, channels, and receptors that are important for intercellular communication (LoTurco and Kriegstein, 1991; Aaku-Saraste et al., 1997), and proliferation (Weissman et al., 2004). The pial fiber of RG cells may also play a role in daughter cell fate determination. Pial fibers make contact with multiple elements in the developing neocortex, including cells in the marginal zone and cortical plate, blood vessels, and migrating neurons, each of which may convey potentially important signaling factors. For example, the association of neural stem cells in the adult hippocampus with blood vessels has led to the suggestion that circulating factors could influence neurogenesis (Palmer et al., 2000; Seri et al., 2004; Shen et al., 2004). The unique morphology of RG cells may permit continuous bidirectional signaling between RG and neighboring VZ cells, migrating daughter cells, and more distant cortical structures. Our demonstration that RG association with migrating daughter cells is uninterrupted by cell cycle dynamics has potential implications not just for migration, but also for fate determination of the dividing RG cell. For example, Notch ligand expression by migrating neurons or migrating IP cells, could activate Notch receptors (Gaiano et al., 2000; Campos et al., 2001), and signal RG cell fate to RG daughter cells. We observed varicosities that travel down the pial fiber and enter the RG soma just before the onset of cytokinesis (see Suppl. Movies 8–10), raising the intriguing possibility that the varicosities represent the transit of signaling information to the RG cell. In this way inheritance of the pial fiber may directly impart an astroglial fate on nascent daughter cells that inherit the pial process.

We find that the only mitotic cells that undergo IKM have bipolar RG cell morphology. We did not observe short VZ progenitor cells (VZ neuroepithelial cells that lack the pial fiber) undergoing IKM, as has been reported (Gal et al., 2006). Our time-lapse studies show that the RG pial fiber is maintained throughout the cell cycle, but becomes very thin during M-phase. In some cases increased laser power or increased image contrast was required to detect this fine process (see Suppl. Movies 2, 8, 9, and 10). Mitotic RG markers such as 4A4 also show that M-phase RG often have very fine, wispy membranes that bridge the radial fiber with the cell body (Noctor et al., 2002). The fine pial processes do not always follow a direct course to the pial surface. They can follow a curving trajectory not restrained to a single plane (see Fig. 3 in Noctor et al., 2007; see Fig. 4 in Weissman et al., 2003), and would be difficult to trace in ultrathin slice preparations. The retrovirus we use should have allowed us to visualize short VZ progenitor cells if they were present. Furthermore, we used low retroviral titers, which labeled single eGFP+ cells in the proliferative zones that were not obscured by adjacent, similarly labeled cells. This approach should allow for a more complete determination of single cell morphology than would be possible using methods that produce dense fields of similarly labeled cells.

We find that RG divisions at the ventricle produce IP cells and that the IP daughter cells maintain contact with the ventricle for several hours after being generated. During peak periods of neurogenesis (e.g., E15 in the rat) IP cells constitute a sizable proportion of mitotic cells within the VZ (see Fig. 7B). IP cells possess a short leading process rather than a pial fiber (see Fig. 4), suggesting that they could potentially be identified as short progenitor cells in the VZ in the absence of labeling techniques that distinguish RG and IP cells. However, a distinguishing feature of IP cells is that they do not exhibit IKM, which is perhaps the definitive hallmark of neuroepithelial cells (Sauer, 1935; Boulder Committee, 1970; Takahashi et al., 1993). During early stages of cortical devel-

opment we observed symmetric proliferative RG divisions that apparently produced two RG daughter cells. Since one daughter cell inherits the RG pial process during division, it follows that the second RG cell produced by symmetric divisions must grow a new fiber, and could therefore appear to be a short progenitor cell until the new pial process has reached the pia. Future studies should examine the dynamics of symmetric RG cell divisions, particularly during early stages of cortical development, to understand how and when these cells acquire RG cell morphology, the degree to which these symmetric daughter cells share each other's characteristics, and how this impacts their generative potential.

Radial glia are neural stem cells

We provide evidence in situ that RG cells possess key characteristics of neural stem cells, including the capacity for self-renewing divisions and the production of multiple cell types. Our classification of RG cell divisions as self-renewing is based on the maintenance of unique identifying characteristics by the RG daughter cells, including bipolar morphology, maintenance of the pial fiber, IKM, and division at the ventricular surface (Misson et al., 1988; Noctor et al., 2001). We find that these features are maintained through multiple divisions within a single RG cell lineage. Recent observations of ES-derived neural stem cells in vitro show that they bear a striking resemblance to RG cells, including spindle-shaped morphology, the potential for self-renewing divisions, expression of RG markers, and interkinetic nuclear movements (Perrier et al., 2004; Conti et al., 2005), suggesting that these properties may be essential, or closely associated with stem cells.

The RG divisions that we classify as self-renewing could actually represent the progression of cortical RG cells along a differentiation pathway, rather than strictly defined self-renewing divisions that produce identical RG daughter cells. For example, sequential RG divisions may produce daughter cells that retain RG morphology, but could differ in the expression of transcription factors associated with different laminar fates (reviewed in Kriegstein et al., 2006). Previous work has identified transcription factors, such as Otx1, that are temporarily expressed in the VZ during the production of specific populations of cortical neurons (Frantz et al., 1994), and heterochronic transplant experiments suggest that commitment to laminar fate may be determined by cell cycle events (McConnell, 1988). In this way the sequential expression of transcription factors by precursor cells in the mammalian neocortex might be analogous to the sequential expression of different genes by *Drosophila* precursor cells during the production of distinct neuroblasts (Brody and Odenwald, 2005; Kriegstein et al., 2006). We also demonstrate that RG cells are multipotential, generating at least four distinct cell types that include additional RG cells, IP cells, neurons, and astroglial cells. The demonstration that RG cells undergo self-renewing divisions while generating multiple cell types in situ indicates that RG cells are likely the neural stem cells that have been described in dissociated cell culture experiments (e.g., Shen et al., 2004). Furthermore, these observations support the notion that the embryonic VZ is largely a niche for self-renewing stem cell divisions, and that the embryonic SVZ is a niche for restricted progenitor cell divisions that amplify specific cortical cell populations (Noctor et al., 2004). Thus, RG and IP cells are analogous to the neurogenic astrocytes and transit amplifying cells that reside in the postnatal and adult SVZ (Alvarez-Buylla and Lim, 2004). The identification and localization of embryonic neural stem cells in situ should advance our understanding of the factors that regulate stem cell behavior, and has potential implications for the application of stem cell biology to disease treatment.

ACKNOWLEDGMENTS

We thank William Walantus, Winston Wong, Jeanelle Agudelo, and Joy Mirjahangir for technical assistance; Drs. Theo Palmer and Fred Gage for generously providing the stably transfected packaging cell line for eGFP-expressing retrovirus, and Dr. Robert Hevner for kindly providing the Tbr2 antibody. We thank members of the Kriegstein lab, Drs. Arturo Alvarez-Buylla, Stewart Anderson, and Corey Harwell for helpful comments on the article.

LITERATURE CITED

Aaku-Saraste E, Oback B, Hellwig A, Huttner WB. 1997. Neuroepithelial cells downregulate their plasma membrane polarity prior to neural tube closure and neurogenesis. Mech Dev 69:71–81.

Adams RJ. 1996. Metaphase spindles rotate in the neuroepithelium of rat cerebral cortex. J Neurosci 16:7610–7618.

Alvarez-Buylla A, Lim DA. 2004. For the long run: maintaining germinal niches in the adult brain. Neuron 41:683–686.

Bayer SA, Altman J. 1991. Neocortical development. New York: Raven Press.

Betschinger J, Knoblich JA. 2004. Dare to be different: asymmetric cell division in Drosophila, C. elegans and vertebrates. Curr Biol 14:R674–685.

Boulder Committee. 1970. Embryonic vertebrate central nervous system: revised terminology. Anat Record 166:257–261.

Brody T, Odenwald WF. 2005. Regulation of temporal identities during Drosophila neuroblast lineage development. Curr Opin Cell Biol 17: 672–675.

Brown JP, Couillard-Despres S, Cooper-Kuhn CM, Winkler J, Aigner L, Kuhn HG. 2003. Transient expression of doublecortin during adult neurogenesis. J Comp Neurol 467:1–10.

Burns JC, Friedmann T, Driever W, Burrascano M, Yee JK. 1993. Vesicular stomatitis virus G glycoprotein pseudotyped retroviral vectors: concentration to very high titer and efficient gene transfer into mammalian and nonmammalian cells. Proc Natl Acad Sci U S A 90:8033–8037.

Cai L, Hayes NL, Takahashi T, Caviness VS Jr, Nowakowski RS. 2002. Size distribution of retrovirally marked lineages matches prediction from population measurements of cell cycle behavior. J Neurosci Res 69:731–744.

Campos LS, Duarte AJ, Branco T, Henrique D. 2001. mDll1 and mDll3 expression in the developing mouse brain: role in the establishment of the early cortex. J Neurosci Res 64:590–598.

Carney RS, Bystron I, Lopez-Bendito G, Molnar Z. 2007. Comparative analysis of extra-ventricular mitoses at early stages of cortical development in rat and human. Brain Struct Funct 212:37–54.

Chenn A, McConnell SK. 1995. Cleavage orientation and the asymmetric inheritance of Notch1 immunoreactivity in mammalian neurogenesis. Cell 82:631–641.

Chenn A, Walsh CA. 2002. Regulation of cerebral cortical size by control of cell cycle exit in neural precursors. Science 297:365–369.

Conti L, Pollard SM, Gorba T, Reitano E, Toselli M, Biella G, Sun Y, Sanzone S, Ying QL, Cattaneo E, Smith A. 2005. Niche-independent symmetrical self-renewal of a mammalian tissue stem cell. PLoS Biol 3:e283.

Das T, Payer B, Cayouette M, Harris WA. 2003. In vivo time-lapse imaging of cell divisions during neurogenesis in the developing zebrafish retina. Neuron 37:597–609.

deAzevedo LC, Fallet C, Moura-Neto V, Daumas-Duport C, Hedin-Pereira

C, Lent R. 2003. Cortical radial glial cells in human fetuses: depth-correlated transformation into astrocytes. J Neurobiol 55:288–298.

des Portes V, Pinard JM, Billuart P, Vinet MC, Koulakoff A, Carrie A, Gelot A, Dupuis E, Motte J, Berwald-Netter Y, Catala M, Kahn A, Beldjord C, Chelly J. 1998. A novel CNS gene required for neuronal migration and involved in X-linked subcortical laminar heterotopia and lissencephaly syndrome. Cell 92:51–61.

Doe CQ. 1996. Asymmetric cell division and neurogenesis. Curr Opin Genet Dev 6:562–566.

Englund C, Fink A, Lau C, Pham D, Daza RA, Bulfone A, Kowalczyk T, Hevner RF. 2005. Pax6, Tbr2, and Tbr1 are expressed sequentially by radial glia, intermediate progenitor cells, and postmitotic neurons in developing neocortex. J Neurosci 25:247–251.

Frantz GD, Weimann JM, Levin ME, McConnell SK. 1994. Otx1 and Otx2 define layers and regions in developing cerebral cortex and cerebellum. J Neurosci 14:5725–5740.

Fujita S. 1960. Mitotic pattern and histogenesis of the central nervous system. Nature 185:702–703.

Gaiano N, Nye JS, Fishell G. 2000. Radial glial identity is promoted by Notch1 signaling in the murine forebrain. Neuron 26:395–404.

Gal JS, Morozov YM, Ayoub AE, Chatterjee M, Rakic P, Haydar TF. 2006. Molecular and morphological heterogeneity of neural precursors in the mouse neocortical proliferative zones. J Neurosci 26:1045–1056.

Gleeson JG, Allen KM, Fox JW, Lamperti ED, Berkovic S, Scheffer I, Cooper EC, Dobyns WB, Minnerath SR, Ross ME, Walsh CA. 1998. Doublecortin, a brain-specific gene mutated in human X-linked lissencephaly and double cortex syndrome, encodes a putative signaling protein. Cell 92:63–72.

Hamilton A. 1901. The division of differentiated cells in the central nervous system of the white rat. J Comp Neurol 11(4):297–322.

Haubensak W, Attardo A, Denck W, Huttner WB. 2004. Neurons arise in the basal neuroepithelium of the early mammalian telencephalon: a major site of neurogenesis. Proc Natl Acad Sci USA 101(9):3196–3201.

Haydar TF, Ang E Jr, Rakic P. 2003. Mitotic spindle rotation and mode of cell division in the developing telencephalon. Proc Natl Acad Sci U S A 100:2890–2895.

Hinds JW, Ruffett TL. 1971. Cell proliferation in the neural tube: an electron microscopic and Golgi analysis in the mouse cerebral vesicle. Z Zellforsch Mikrosk Anat 115:226–264.

Huttner WB, Brand M. 1997. Asymmetric division and polarity of neuroepithelial cells. Curr Opin Neurobiol 7:29–39.

Kamei Y, Inagaki N, Nishizawa M, Tsutsumi O, Taketani Y, Inagaki M. 1998. Visualization of mitotic radial glial lineage cells in the developing rat brain by Cdc2 kinase-phosphorylated vimentin. Glia 23:191–199.

Kempermann G, Jessberger S, Steiner B, Kronenberg G. 2004. Milestones of neuronal development in the adult hippocampus. Trends Neurosci 27:447–452.

Kosodo Y, Roper K, Haubensak W, Marzesco AM, Corbeil D, Huttner WB. 2004. Asymmetric distribution of the apical plasma membrane during neurogenic divisions of mammalian neuroepithelial cells. EMBO J 23:2314–2324.

Kriegstein AR, Götz M. 2003. Radial glia diversity: a matter of cell fate. Glia 43:37–43.

Kriegstein A, Noctor S, Martínez-Cerdeño V. 2006. Patterns of neural stem and progenitor cell division may underlie evolutionary cortical expansion. Nat Rev Neurosci 7:883–890.

Landrieu P, Goffinet A. 1979. Mitotic spindle fiber orientation in relation to cell migration in the neo-cortex of normal and reeler mouse. Neurosci Lett 13:69–72.

Langman J, Guerrant RL, Freeman BG. 1966. Behavior of neuro-epithelial cells during closure of the neural tube. J Comp Neurol 127:399–411.

LoTurco JJ, Kriegstein AR. 1991. Clusters of coupled neuroblasts in embryonic neocortex. Science 252:563–566.

LoTurco JJ, Sarkisian MR, Cosker L, Bai J. 2003. Citron kinase is a regulator of mitosis and neurogenic cytokinesis in the neocortical ventricular zone. Cereb Cortex 13:588–591.

Lyons DA, Guy AT, Clarke JD. 2003. Monitoring neural progenitor fate through multiple rounds of division in an intact vertebrate brain. Development 130:3427–3436.

Martin AH. 1967. Significance of mitotic spindle fibre orientation in the neural tube. Nature 216:1133–1134.

Mayer B, Emery G, Berdnik D, Wirtz-Peitz F, Knoblich JA. 2005. Quantitative analysis of protein dynamics during asymmetric cell division. Curr Biol 15:1847–1854.

McConnell SK. 1988. Fates of visual cortical neurons in the ferret after isochronic and heterochronic transplantation. J Neurosci 8:945–974.

Mione MC, Cavanagh JFR, Harris B, Parnavelas JG. 1997. Cell fate specification and symmetrical/asymmetrical divisions in the developing cerebral cortex. J Neurosci 17:2018–2029.

Misson JP, Edwards MA, Yamamoto M, Caviness VS Jr. 1988. Mitotic cycling of radial glial cells of the fetal murine cerebral wall: a combined autoradiographic and immunohistochemical study. Brain Res 466:183–190.

Miyata T, Kawaguchi A, Okano H, Ogawa M. 2001. Asymmetric inheritance of radial glial fibers by cortical neurons. Neuron 31:727–741.

Miyata T, Kawaguchi A, Saito K, Kawano M, Muto T, Ogawa M. 2004. Asymmetric production of surface-dividing and non-surface-dividing cortical progenitor cells. Development 131(13):3133–3145.

Noctor SC, Flint AC, Weissman TA, Dammerman RS, Kriegstein AR. 2001. Neurons derived from radial glial cells establish radial units in neocortex. Nature 409:714–720.

Noctor SC, Flint AC, Weissman TA, Wong WS, Clinton BK, Kriegstein AR. 2002. Dividing precursor cells of the embryonic cortical ventricular zone have morphological and molecular characteristics of radial glia. J Neurosci 22:3161–3173.

Noctor SC, Martínez-Cerdeño V, Ivic L, Kriegstein AR. 2004. Cortical neurons arise in symmetric and asymmetric division zones and migrate through specific phases. Nat Neurosci 7:136–144.

Noctor SC, Martinez-Cerdeno V, Kriegstein AR. 2007. Neural stem and progenitor cells in cortical development. In: Parnavelas JG, editor. Cortical development: genes and genetic abnormalities. Chichester: Wiley, Novartis Foundation Symposium 288.

Palmer TD, Markakis EA, Willhoite AR, Safar F, Gage FH. 1999. Fibroblast growth factor-2 activates a latent neurogenic program in neural stem cells from diverse regions of the adult CNS. J Neurosci 19:8487–8497.

Palmer TD, Willhoite AR, Gage FH. 2000. Vascular niche for adult hippocampal neurogenesis. J Comp Neurol 425:479–494.

Pelvig DP, Pakkenberg H, Stark AK, Pakkenberg B. 2007. Neocortical glial cell numbers in human brains. Neurobiol Aging (in press).

Perrier AL, Tabar V, Barberi T, Rubio ME, Bruses J, Topf N, Harrison NL, Studer L. 2004. Derivation of midbrain dopamine neurons from human embryonic stem cells. Proc Natl Acad Sci U S A 101:12543–12548.

Peters A, Jones EG. 1984. Cerebral cortex. In: Jones EG, Peters A, editors. Cerebral cortex. New York: Plenum Press. p 107–121.

Poggi L, Vitorino M, Masai I, Harris WA. 2005. Influences on neural lineage and mode of division in the zebrafish retina in vivo. J Cell Biol 171:991–999.

Privat A. 1975. Postnatal gliogenesis in the mammalian brain. Int Rev Cytol 40:281–323.

Quinn JC, Molinek M, Martynoga BS, Zaki PA, Faedo A, Bulfone A, Hevner RF, West JD, Price DJ. 2007. Pax6 controls cerebral cortical cell number by regulating exit from the cell cycle and specifies cortical cell identity by a cell autonomous mechanism. Dev Biol 302:50–65.

Reid CB, Tavazoie SF, Walsh CA. 1997. Clonal dispersion and evidence for asymmetric cell division in ferret cortex. Development 124:2441–2450.

Reznikov K, Acklin SE, van der Kooy D. 1997. Clonal heterogeneity in the early embryonic rodent cortical germinal zone and the separation of subventricular from ventricular zone lineages. Dev Dyn 210:328–343.

Sanada K, Tsai LH. 2005. G protein betagamma subunits and AGS3 control spindle orientation and asymmetric cell fate of cerebral cortical progenitors. Cell 122:119–131.

Sauer FC. 1935. Mitosis in the neural tube. J Comp Neurol 62:377–405.

Schaar BT, Kinoshita K, McConnell SK. 2004. Doublecortin microtubule affinity is regulated by a balance of kinase and phosphatase activity at the leading edge of migrating neurons. Neuron 41:203–213.

Schmechel DE, Rakic P. 1979. A Golgi study of radial glial cells in developing monkey telencephalon: morphogenesis and transformation into astrocytes. Anat Embryol 156:115–152.

Seri B, Garcia-Verdugo JM, Collado-Morente L, McEwen BS, Alvarez-Buylla A. 2004. Cell types, lineage, and architecture of the germinal zone in the adult dentate gyrus. J Comp Neurol 478:359–378.

Shen Q, Zhong W, Jan YN, Temple S. 2002. Asymmetric Numb distribution is critical for asymmetric cell division of mouse cerebral cortical stem cells and neuroblasts. Development 129:4843–4853.

Shen Q, Goderie SK, Jin L, Karanth N, Sun Y, Abramova N, Vincent P, Pumiglia K, Temple S. 2004. Endothelial cells stimulate self-renewal and expand neurogenesis of neural stem cells. Science 304:1338–1340.

Smart IH. 1961. The subependymal layer of the mouse brain and its cell production as shown by radioautography after thymidine-H3 injection. J Comp Neurol 116:325–345.

Smart IH. 1973. Proliferative characteristics of the ependymal layer during the early development of the mouse neocortex: a pilot study based on recording the number, location and plane of cleavage of mitotic figures. J Anat 116:67–91.

Smart IH, Dehay C, Giroud P, Berland M, Kennedy H. 2002. Unique morphological features of the proliferation zones and postmitotic compartments of the neural epithelium giving rise to striate and extrastriate cortex in the monkey. Cereb Cortex 12(1):37–53.

Takahashi T, Nowakowski RS, Caviness V Jr. 1993. Cell cycle parameters and patterns of nuclear movement in the neocortical proliferative zone of the fetal mouse. J Neurosci 13:820–833.

Takahashi T, Nowakowski RS, Caviness V Jr. 1995a. Early ontogeny of the secondary proliferative population of the embryonic murine cerebral wall. J Neurosci 15:6058–6068.

Takahashi T, Nowakowski RS, Caviness V Jr. 1995b. The cell cycle of the pseudostratified ventricular epithelium of the embryonic murine cerebral wall. J Neurosci 15:6046–6057.

Tanaka T, Serneo FF, Higgins C, Gambello MJ, Wynshaw-Boris A, Gleeson JG. 2004. Lis1 and doublecortin function with dynein to mediate coupling of the nucleus to the centrosome in neuronal migration. J Cell Biol 165:709–721.

Tarabykin V, Stoykova A, Usman N, Gruss P. 2001. Cortical upper layer neurons derive from the subventricular zone as indicated by Svet1 gene expression. Development 128:1983–1993.

Tibber MS, Kralj-Hans I, Savage J, Mobbs PG, Jeffery G. 2004. The orientation and dynamics of cell division within the plane of the developing vertebrate retina. Eur J Neurosci 19:497–504.

Walsh C, Cepko CL. 1988. Clonally related cortical cells show several migration patterns. Science 241:1342–1345.

Walsh C, Cepko CL. 1992. Widespread dispersion of neuronal clones across functional regions of the cerebral cortex. Science 255:434–440.

Weissman T, Noctor SC, Clinton BK, Honig LS, Kriegstein AR. 2003. Neurogenic radial glial cells in reptile, rodent and human: from mitosis to migration. Cereb Cortex 13:550–559.

Weissman TA, Riquelme PA, Ivic L, Flint AC, Kriegstein AR. 2004. Calcium waves propagate through radial glial cells and modulate proliferation in the developing neocortex. Neuron 43:647–661.

Wodarz A. 2005. Molecular control of cell polarity and asymmetric cell division in Drosophila neuroblasts. Curr Opin Cell Biol 17:475–481.

Zamenhof S. 1985. Quantitative studies of mitoses in cerebral hemispheres of fetal rats. Brain Res 352:306–309.

Zamenhof S. 1987. Quantitative studies of mitoses in fetal rat brain: orientations of the spindles. Brain Res 428:143–146.

Zhong W, Feder JN, Jiang MM, Jan LY, Jan YN. 1996. Asymmetric localization of a mammalian numb homolog during mouse cortical neurogenesis. Neuron 17:43–53.

Zolessi FR, Poggi L, Wilkinson CJ, Chien CB, Harris WA. 2006. Polarization and orientation of retinal ganglion cells in vivo. Neural Dev 1:2.